Assessing Deterioration of an In-field RC Bridge Deck by AE Tomography

M. Fukuda, K.C. Chang, H. Nakayama, H. Asaue, T. Nishida, T. Shiotani, T. Miyagawa, K. Watabe, and T. Oshiro

Abstract Deterioration of aging infrastructures is an important issue in many developing and well-developed countries. For maintenance of the infrastructures in limited budgets, proactive inspections and countermeasures are important before severe structural damage occurs. To assess the deterioration of those structures in a reliable and preferably nondestructive manner is highly demanded. Responding to the demand, acoustic emission (AE) tomography can be regarded as a powerful method since it builds the elastic-wave velocity distribution of the medium that AE waves propagate through while simultaneously locating AE sources. Such a method has been widely tested in laboratories but not yet fully realized in fields. In the present study, the applicability of two-dimensional (2D) and three-dimensional (3D) AE tomography techniques to the evaluation of internal damages in existing RC bridge deck was examined using the data obtained by single-side AE measurement. The overlay of 2D elastic-wave velocity distribution with AE source locations reveals that AE was active in moderate-velocity areas and the boundaries of low-velocity areas, which were regarded as deteriorated areas with progressing defects. Moreover, in the AE measurement, a large number of AE with small amplitudes were observed in the severely deteriorated panel; amazingly, primary AEs were captured, which implied the propagation of an internal crack in the deck.

M. Fukuda • T. Oshiro
West Nippon Expressway Company Limited, 1-6-20 Dojima Kita, Osaka, Japan
e-mail: m.fukuda.ac@w-nexco.co.jp

K.C. Chang • H. Nakayama • H. Asaue • T. Nishida (✉) • T. Shiotani • T. Miyagawa
Kyoto University, Nishikyo, Kyoto, Japan
e-mail: nishida.takahiro.6e@kyoto-u.ac.jp; shiotani.tomoki.2v@kyoto-u.ac.jp

K. Watabe
Toshiba Corporation, Komukaitoshiba 1, saiwai, Kawasaki, Kanagawa, Japan
e-mail: kazuo.watabe@toshiba.co.jp

G. Shen et al. (eds.), *Advances in Acoustic Emission Technology*, Springer Proceedings in Physics 179, DOI 10.1007/978-3-319-29052-2_25

1 Introduction

Recently, deterioration of aging infrastructures like RC bridge decks is becoming a major concern around the world. As available budgets and manpower are always limited, effective maintenance of infrastructures is highly demanded. Proactive inspections and countermeasures are important before severe structural damage occurs. In addition to the conventional visual inspections, nondestructive testing techniques that can evaluate interior damage of the infrastructures are widely investigated. Here acoustic emission (AE) tomography can be regarded as one of the efficient nondestructive testing techniques mentioned above [1]. In the visualized velocity distribution, lower-velocity zones may indicate deteriorated areas in acknowledging the fact that damage like cracks or voids in concrete structures may force elastic waves bypass and therefore decrease their observed velocities. Such a method has been widely tested in laboratories but not yet fully realized in fields [2, 3].

In the present study, the applicability of two-dimensional (2D) and three-dimensional (3D) AE tomography techniques to the evaluation of internal damages in existing RC bridge deck was examined using the data obtained by single-side AE measurement. In addition, basic evaluations based on AE parameters are implemented.

2 Outline of AE Measurement in Actual RC Deck

The surface condition of the target RC deck is shown in Fig. 1. This RC deck is supported by steel girder and has been served for 40 years as a part of a highway in Nara Prefecture, Japan.

AE measurement system is AMSY-6 MB19 by Vallen Systeme GmbH. Twelve AE sensors of 30 kHz resonant frequency (VS30-V by Vallen Systeme GmbH) were installed on the bottom surface of the highway bridge deck, 6 on the panel severely deteriorated (upper panel in Fig. 1) and 6 on another panel slightly deteriorated (lower panel) by visual inspection. AE activities under normal traffic loadings were monitored from 10:08 AM, 24th Dec., 2014 to 9:28 AM, 26th Dec., 2014 and a total of 29,438,265 AE events were acquired. Most of AE data obtained in-situ measurements are secondary AE induced by traffic loads. The relationship between the AE peak amplitude and LUCY (Location Uncertainty, defined in VisualAE®) [4] is shown in Fig. 2. It shows that as the peak amplitude increases, the number of AE events and LUCY decrease. Herein, the threshold was set as 60 dB for peak amplitude and 0.3 m (half of sensor spacing) for LUCY, i.e., AE events with peak amplitude smaller than 60 dB and a LUCY larger than 0.3 m are filtered out for further analysis.

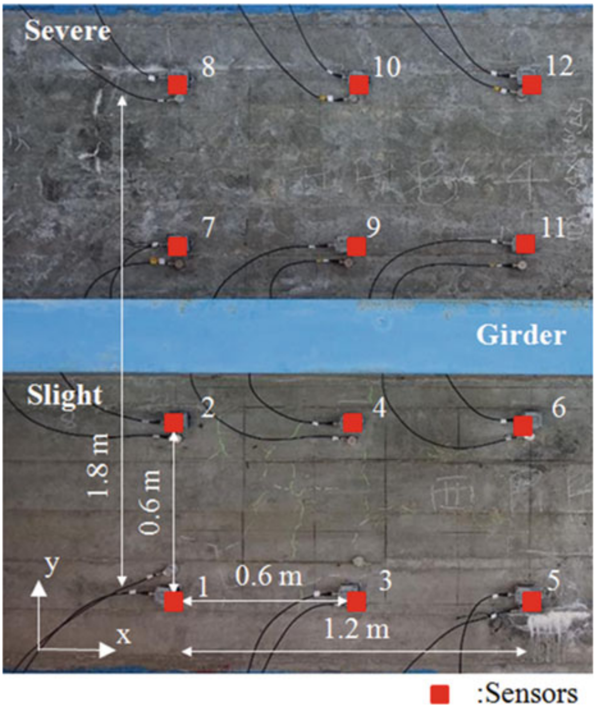

Fig. 1 Target RC deck and sensor layout

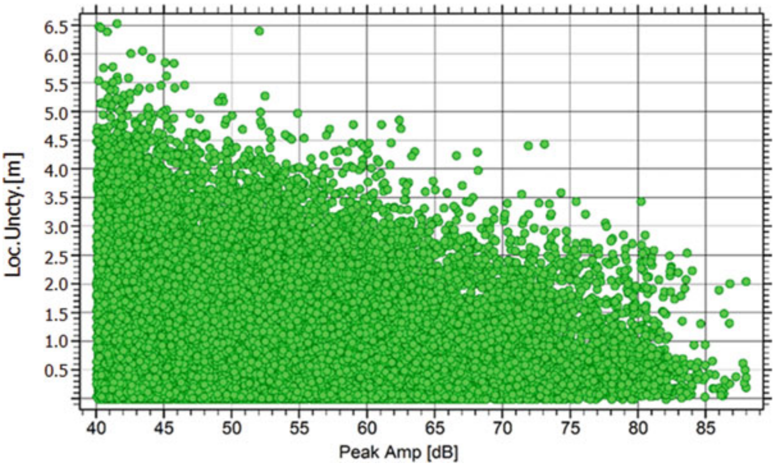

Fig. 2 Relation between peak amplitude and LUCY

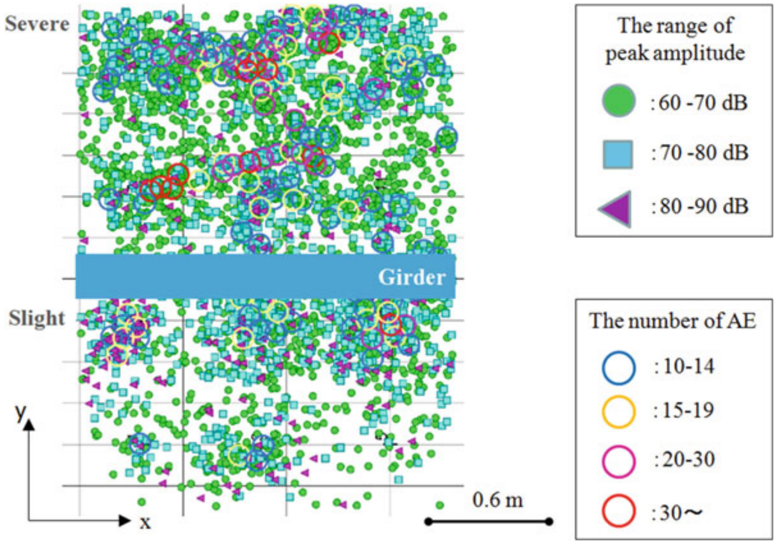

Fig. 3 AE source locations

3 AE Analysis

3.1 Source Location Analysis

AE source locations are shown in Fig. 3, where the AE peak amplitudes are labeled as follows: 60–70 dB in green circle, 70–80 dB blue square, and 80–90 dB in purple triangle. Also, the numbers of AE events clustering in a circular area of 0.1 m in diameter are marked in hollow circles as follows: 10–14 events in blue, 15–19 events in yellow, 20–30 events in pink, and more than 29 events in red. It is observed that AE activities were denser and generally of smaller peak amplitude in the severely deteriorated panel than the slightly deteriorated panel.

3.2 Crack Propagation Detected in AE Measurement

In order to investigate the AE source locations in detail, the measured area was divided into small area of 0.1 m × 0.1 m and AE sources were counted for each area. Among those small areas, we were interested in a specific area where extraordinarily many AE events (383 in number) were captured. The cumulative number of AE events in this area is shown in Fig. 4a, where the full time-span was separated into 5 intervals: Interval 1 is from 10:00, 24th Dec. to 18:30, 25th Dec., Interval 2 is from 18:30 to 20:20, 25th Dec., Interval 3 is from 20:20 to 22:30, 25th Dec., Interval 4 is from 22:30, 25th Dec. to 1:30, 26th Dec., and Interval 5 is from

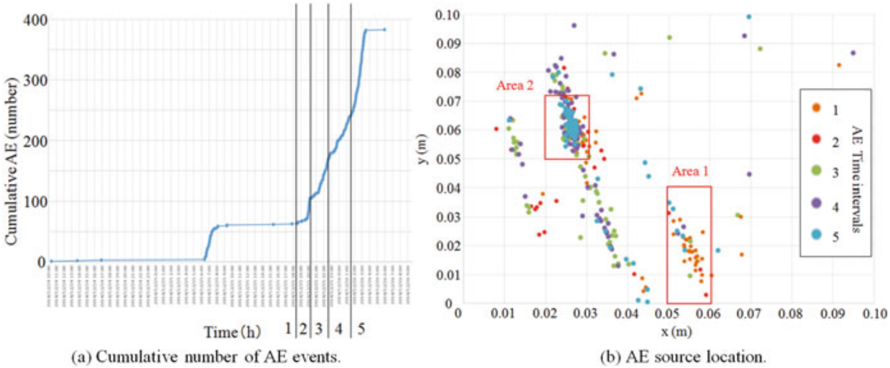

Fig. 4 AE events in a specific 0.1 m × 0.1 m area. (**a**) Cumulative number of AE events. (**b**) AE source location

1:30 to 9:28, 26th Dec. In this area, AE occurred from 6:00 to 9:00, 25th Dec. (in Interval 1 of Fig. 4a), calmed down once and then occurred continuously from 18:30, 25th Dec. to 3:30, 26th Dec. (intervals 2–5).

The AE sources location is shown in Fig. 4b. Amazingly the majority of the sources distributed in two belt zones. Let us take a closer look at Area 1 (x = 0.05–0.06 m, y = 0–0.04 m, Fig. 4b) and Area 2 (x = 0.02–0.03 m, y = 0.05–0.07 m). In Area 1, a large number of AE events were observed in Interval 1. In Area 2, AE events were observed continuously in all intervals and they extended towards upper-left side of this area. Although the frequency characteristics or other AE parameters have not been comprehensively studied yet, the rapidly increasing number (Fig. 4a) and spatial concentration (Fig. 4b) of AE events in Area 2 might imply a propagating internal crack, which released primary AE waves.

4 2D AE Location and Elastic Wave Velocity Distribution

Elastic wave tomography analysis (see [1, 2] for detailed algorithm) was also implemented using hammering impacts. Area of tomography analysis and hammering points are shown in Fig. 5. In the elastic wave tomography analysis, velocity distribution of surface or measured media is acquired. It is known that the velocities tend to be high when the media is uniform and sound. The elastic wave velocity distribution overlaid with AE sources location is plotted in Fig. 6. It is observed that AE of large amplitude occurred at moderate-velocity areas (3300–3800 m/s) and the boundaries of low-velocity areas (3300 m/s or lower); fewer AE occurred at high-velocity areas (4100 m/s and higher) and low-velocity areas.

This observation can be explained in mechanical sense as follows. In high-velocity areas, which are generally regarded as sound areas, AEs are inactive and

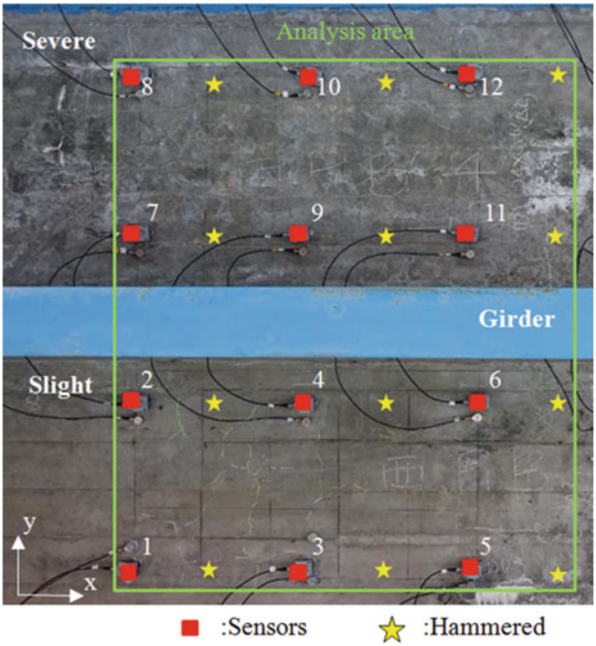

Fig. 5 Area of tomography analysis and hammering points

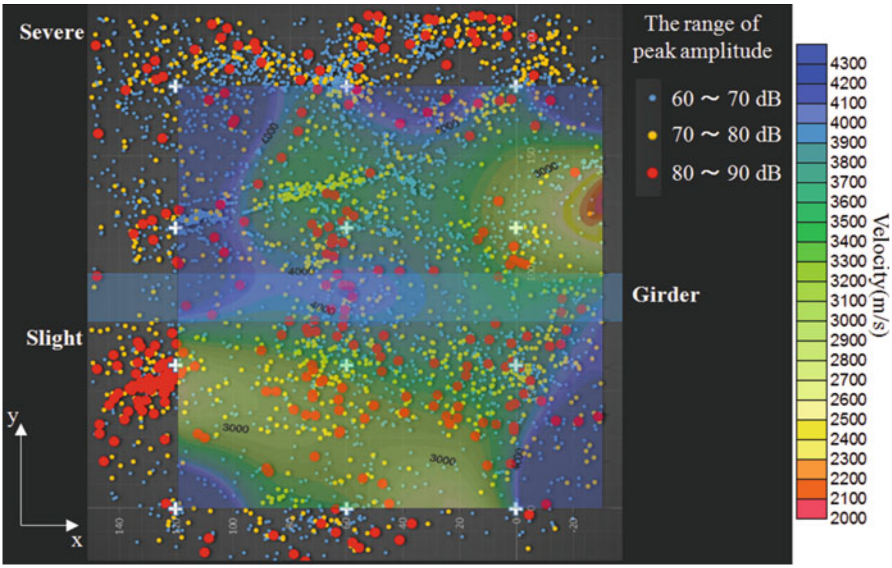

Fig. 6 Comparison of AE location and elastic wave velocity

their amplitudes are small because there are little defects causing internal frictions. It means that crack interface is mostly contact in this area. Therefore, this result indicates less defects area. In the low-velocity areas, which are regarded as highly deteriorated areas, AEs are inactive as well since the defects like cracks have fully developed and little new defects propagating. This area can be estimated as crack interface with less contact; AEs are difficult to generate because of less friction. The area is regarded as a defected area.

As for the moderate-velocity areas and the boundaries low-velocity areas, AEs are active and their amplitudes are large due to the propagation and frictions of newly developing defects. It is estimated that the results of velocity structures indicate edge of clacks. AEs are easy to generate in the area because clacks will make progress at this area. Fatigue damage by traffic load has been progressing during the measurement.

5 3D AE Tomography Analysis

A 3D AE tomography was performed, using the obtained AE events. The same area as that for 2D analysis as shown in Fig. 7 was considered, which is confined by the sensors No. 1, 5, 8, and 12. The area was discretized into $6 \times 8 \times 2$ meshes in the $X \times Y \times Z$ dimensions. Forty AE events that had large amplitude and were measured by at least four sensors at the same event were used for the 3D AE tomography analysis, to obtain 3D AE source locations and elastic wave velocity distribution. AE sources located by 3D AE tomography analysis are compared with those by 2D AE tomography analysis, as shown in Fig. 7. From these results, it could be said that similar source locations were identified in 2D and 3D analysis. 3D analysis is more powerful in that AE sources can be located inside the deck.

3D elastic wave velocity distribution from 3D AE tomography analysis is shown in Fig. 8, where variations of the internal velocity can be observed. The elastic wave velocity distributions extracted at the horizontal planes $z = -0.05$ and -0.15 m are shown in Fig. 9. Near the bottom surface of the deck ($z = -0.05$ m), low velocity areas were observed and those areas were considered as deteriorated areas. On the other hand, at the plane $z = -0.15$ m, high velocity was observed in most areas, which indicated the internal deterioration was less progressed than the surface. The velocity distributions at cross-section of $x = 0.45$ m, 0.75 m and $y = -0.45$ m, -1.35 m, are shown in Fig. 10. It was observed that velocity distributions were not uniform in the concrete deck and low velocity (around 2000 m/s) areas were distributed below the depth of 0.1 m measured from the bottom surface (the sensor side). As mentioned above, 3D AE tomography analysis would be able to visualize the interior distribution of concrete quality, which is unavailable by both the 2D AE tomography analysis and conventional visual inspection.

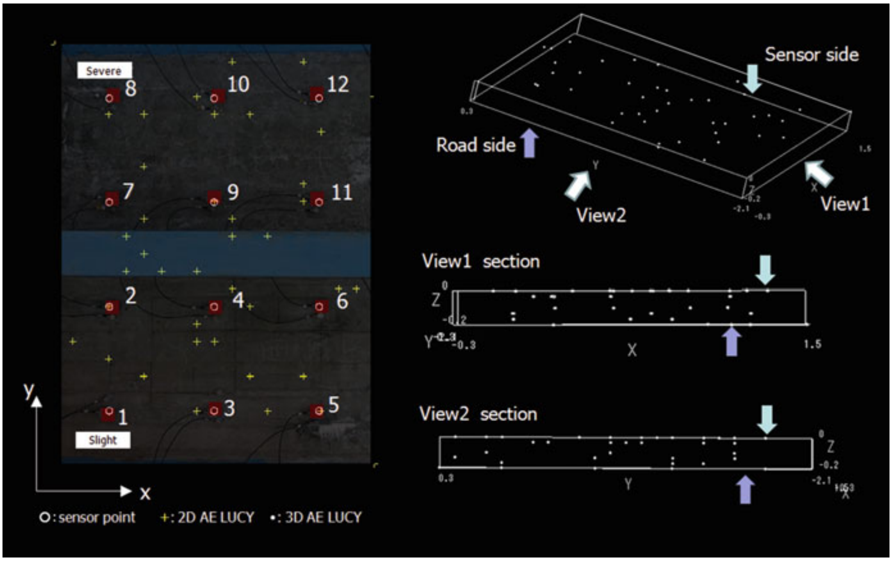

Fig. 7 AE source location detected by 2D and 3D tomography

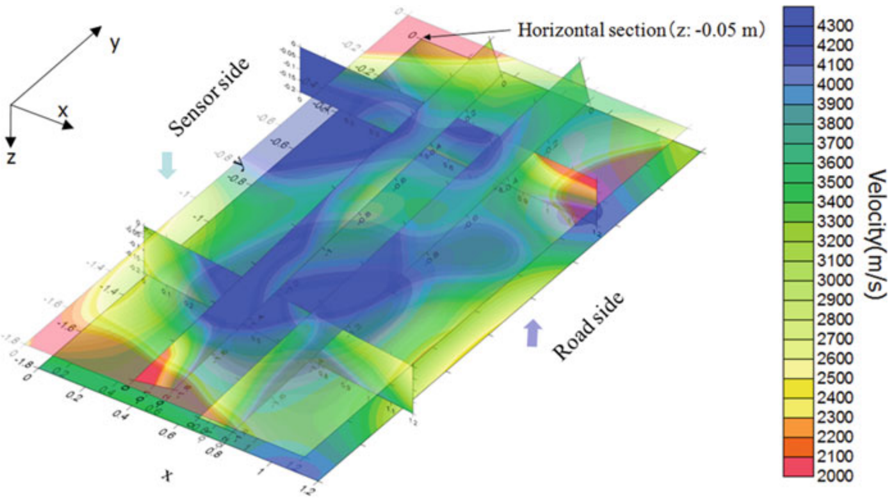

Fig. 8 Panel diagram of 3D analysis

6 Summary

Following conclusions could be drawn from the present experimental study.

1. In the AE measurement on the real RC deck, a large number of AE with small amplitudes were observed in the severely deteriorated panel and a smaller

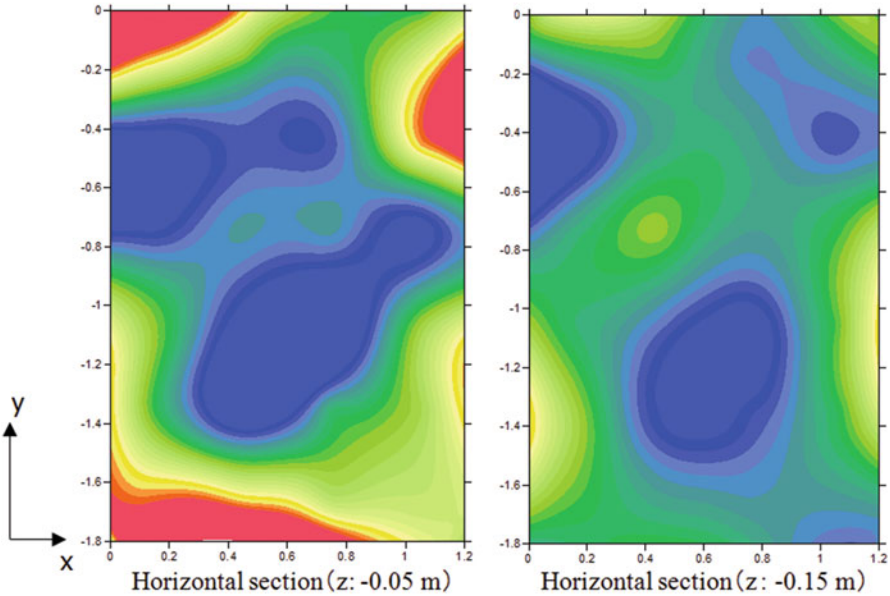

Fig. 9 Elastic wave velocity distribution (z-axis)

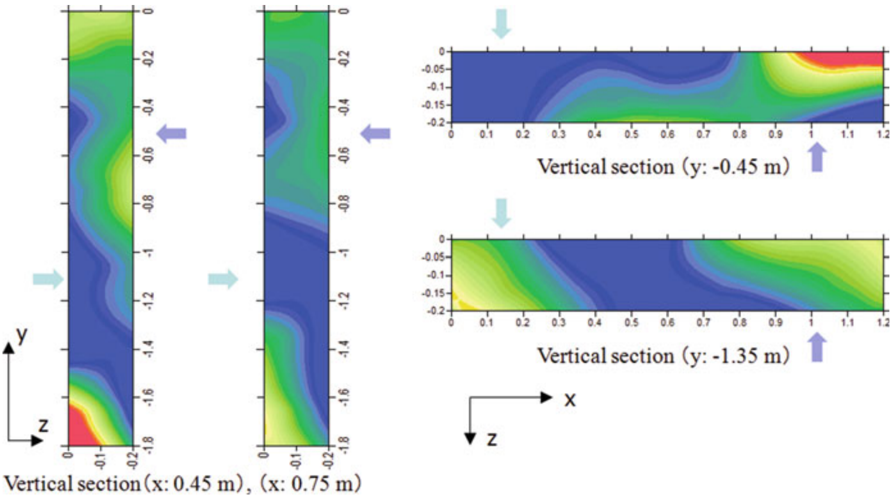

Fig. 10 Elastic wave velocity distribution (x-axis and y-axis)

number of AE with large amplitudes were detected in the slightly deteriorated panel. Amazingly, primary AEs were captured during the measurement, which implied the propagation of an internal crack.

2. The overlay of 2D elastic-wave velocity distribution with AE source locations reveals that AE was active in moderate-velocity areas and the boundaries of

low-velocity areas, which were regarded as deteriorated areas with progressing defects. Contrarily, AE was less active in high- and low-velocity areas, which were regarded as sound areas and deteriorated areas with fully developed defects, respectively.

3. The present AE tomography works well for the in-field RC bridge deck as illustrated above. It is available to assess deteriorations of the target deck in either 2D or 3D elastic-wave velocity distribution, which encourages a further practicability study along this line.

Acknowledgment A part of field measurements was financially supported by NEDO, New Energy and Industrial Technology Development Organization.

References

1. T. Shiotani, D.G. Aggelis, O. Makishima, Global monitoring of large concrete structures using acoustic emission and ultrasonic techniques: case study. J. Bridg. Eng. **14**(3), 188–192 (2009)
2. Kobayashi, Y., Shiotani, T., Oda, K., in *System identification for three-dimensional AE-tomography with Kalman Filter, Proceedings of the 31th Conference of the European Working Group on Acoustic Emission*, 2014
3. Shiotani Tomoki, Okude Nobuhiro, Momoki Shohei, Yoshikazu Kobayashi, in *Proposal of soundness evaluation method for infrastructure construction by AE tomography, Japan Non-destructive Inspection Association, the 18th AE General Conference Papers*, 39–42, 2011 (in Japanese)
4. M.A. Hamstad, Acoustic emission source location in a thick steel plate using lamb modes. J. Acoustic Emission **25**, 194–214 (2007)